Magnon Tunneling Between Two Magnon Bose-Einstein Condensates

A. D. Belanovsky
Crocus Nanoelectronics
P. M. Vetoshko
Kotelnikov Institute of radioengineering and electronics of RAS
Yu. M. Bunkov (y.bunkov@rnf.com)
M-Granat, Russian Quantum Center

Research Article

Keywords: Magnon tunneling, condensates, quantum magnonics, quantum computers, hybrid quantum systems

Posted Date: September 15th, 2021

DOI: https://doi.org/10.21203/rs.3.rs-877928/v1

Magnon tunneling between two magnon Bose-Einstein condensates

A.D. Belanovsky[1], P.M. Vetoshko[2], and Yu.M. Bunkov[3,*]

[1]Crocus Nanoelectronics, Volgogradskiy prospect 42 build. 5, premise 1, Moscow, 109316, Russia
[2]Kotelnikov Institute of radioengineering and electronics of RAS, Mokhovaya str., 11-7, Moscow 125009, Russia
[3]M-Granat, Russian Quantum Center, Skolkovo, Bolshoy Bulvar 30, bld. 1, Moscow, 121205, Russia
[*]y.bunkov@rqc.ru

ABSTRACT

The explosive development of quantum magnonics is explained by its potential of use in quantum computers, processing information and the formation of hybrid quantum systems. The processes of spatial correlation of quantum systems are fundamental and lead to such phenomena as the Josephson effect and superconductivity. In particular, they determine the phenomenon of the magnon superfluidity and magnon Bose condensation which were first discovered in antiferromagnetic superfluid ^{3}He. In this article, we consider the features of magnon Bose condensation in yttrium iron garnet film. We simulate the processes of magnon BEC coherency and magnon tunneling through the gap.

Introduction

Magnetism is a quantum phenomenon whose properties are usually considered in the classical approximation. In this approximation the quantum transitions between the atomic levels are described in terms of the precession of locally averaged magnetization. We should not forget that the basis of spin dynamics lies in the field of quantum mechanics, and their consideration in the form of classical physics is approximate. For example, the well known temperature dependence of magnetization stands out beyond the classical paradigm and is described by the density of magnons. Magnons are a quantum quasiparticles with integer spin which obey Bose statistics. According to the Holstein-Primakoff formalism[1], they correspond to the quantum transition of a single spin, the energy of which is distributed over the ensemble of magnetic moments at a distance of exchange interaction. The density of equilibrium magnons is determined by the temperature. However, we can excite a large number of non-equilibrium magnons by magnetic resonance methods - the deflection of precessing magnetization at radio-frequency (RF) pumping. A great interest attracts the phenomenon of magnon Bose - Einstein condensation (mBEC), which occurs at a sufficient concentration of magnons. The question arose, as a relatively short time living non-equilibrium magnons can form a coherent state? Experimental investigations show that there is a sufficient time of its thermalization among themselves in case of impulse excitation. Moreover, under continuous excitation, a steady mBEC is formed.

It is easy to estimate the relation between the density of non-equilibrium magnons and the angle of magnetization deflection. The number of excited magnons $\hat{N}$ related to the deviation of spin $\hat{S}_z$ from its equilibrium value S[1]:

$$\hat{N} = \hat{a}_0^\dagger \hat{a}_0 = \frac{S - \hat{S}_z}{\hbar} , \tag{1}$$

where $\hat{a}_0^\dagger$ and $\hat{a}_0$ are magnons creation and annihilation operators. As the magnon density increases, it can reach a critical value at which a Bose condensed state formed. The corresponding critical density of magnons for yttrium iron garnet (YIG) was considered in[2] and corresponds to the deviation of precessing magnetization at an angle of about 3°. These phenomena, as well as the quantum transport of magnetization by magnon supercurrent are quantum phenomena and can be considered in the classical approximation with great care. However, according to a widespread concept that for $N \to \infty$ the spin dynamics is approaching classical variables. Consequently, the calculations within the framework of the classical paradigm can be considered as a good approximation, of quantum processes. Possible contradictions between the results of classical calculations and experimental results are of paramount importance for the verification of the quantum properties of magnons. In particular, the existence of quantum entanglement for mBEC is of great interest, since it is a central source in many quantum information protocols, which naturally arise in any study of quantum technologies[3–5].

MBEC properties

BEC states can be described by a macroscopic wave function[6]:

$$\Psi_0(\vec{r},t) = \psi_0(\vec{r}) \exp i(\alpha - \mu t/\hbar), \tag{2}$$

where

$$\mu = \frac{\partial E}{\partial N} \tag{3}$$

is the chemical potential and $\psi_0(\vec{r})$ is real and normalized to the total number of particles N_0,

$$\int d\vec{r} \psi_0^2(\vec{r}) = N_0. \tag{4}$$

The mBEC wave function for time variables reads[7]:

$$\Psi_0(t) = \hat{N}^{1/2} \exp i(\varphi - \Delta\omega t) = \sqrt{\frac{2S}{\hbar}} \sin\frac{\theta}{2} \exp i(\varphi - i\Delta\omega t). \tag{5}$$

where φ and θ are the phase of precession and the angle of magnetization deflection, $\Delta\omega$ is the difference between the Larmor frequency at a small excitation and frequency of mBEC precession. It plays a role of magnon chemical potential of magnon-magnon interaction.

This wave function satisfies a Gross-Pitaevskii equation similarly to other BEC systems[8]

$$i\hbar\frac{\partial\Psi_0}{\partial t} = \left(-\frac{\hbar^2}{2m}\Delta_{\vec{r}} + V(\vec{r}) + g|\Psi_0|^2\right)\Psi_0. \tag{6}$$

where the first term describes the magnetic gradient energy, the second one - potential energy in magnetic field and the third one - the chemical potential of magnon-magnon interaction energy. This nonlinear term leads to frequency shift from the Larmor frequency, which plays a very important role for stability of mBEC and magnon superfluidity. The repulsive interaction between magnons responsible for formation of mexican hat energy potential[7], typical for superconductivity and determines the value of critical supercurrent. In the case of attractive interaction the mBEC state and supercurrent are unstable.

In this article, we consider the out of plane magnetized YIG film, in which the interaction is repulsive, and the frequency increases with magnons density (deviation of magnetization), which reads:

$$\omega = \gamma(H - 4\pi M_S \cos\theta), \tag{7}$$

where M_S is a saturated magnetization. At a small excitation the angle θ is near zero and the frequency of precession corresponds to the Larmor frequency ω_0 in the effective field $(H - 4\pi M_S)$. But at the high excitation the frequency of precession increases on $\Delta\omega = \omega_0(1 - \cos\theta)$ with the magnetization deflection due to magnon interaction.

At a permanent RF pumping the chemical potential of mBEC is determined by the RF frequency, which determines the density of nonequilibrium magnons, and therefore the angle of magnetization deflection. In other words, magnon density is determined by the frequency of excitation, and not on its intensity, while RF power is enough to compensate for magnons relaxation, as shown in[9]. Of course, only a part of non-equilibrium magnons condenses. Indeed, non-condensed magnons must follow mBEC due to interaction between them. This is similar to the case of superfluid ^{4}He, where only a few percent of atoms are Bose condensed, but the density of superfluid component corresponds to 100% of atoms at zero temperature. As a result the magnetic moment of mBEC state is

$$M_{BEC} = \hbar N = S(1 - \cos\theta), \tag{8}$$

Experimental observation of mBEC

MBEC was observed as the spontaneously self-organized phase-coherent precession of magnetization in an antiferromagnetic superfluid ^{3}He-B[10,11]. The formation of the state with coherent precession of magnetization even at a very inhomogeneous magnetic field was explained by magnons supercurrent due to the spatial gradient of phase of precession $\nabla\varphi$[12].

$$J_{BEC} = M_{BEC}\nabla\varphi. \tag{9}$$

There was observed a number of quantum phenomena like a phase-slippage at a critical magnon supercurrent in a long channel[13–15], magnon Josephson effect[16,17] and magnon-current vortices[18,19]. The review of magnon supercurrent and mBEC investigations in ^{3}He can be found in[7,20,21]. The question of magnon entanglement was also investigated in ^{3}He-B. There was observed experimentally the Josephson oscillations between two mBEC states[22].

The existence of quantum magnetic phenomena in quantum superfluid ^{3}He do not cause surprise. However, these phenomena are not directly related to superfluidity of ^{3}He and can be found in other magnetic materials. Thus, mBEC and magnon superfluidity was observed in solid materials, including antiferromagnets with a coupling nuclear electron precession[23–26] and YIG film, magnetized in plane[27,28] and out of plane[9,29].

Many experimental results of mBEC investigations does not contradict the classic model when the mBEC state is viewed in the framework of the macrospin model. Therefore, in this article we use a quasi-classical model assuming that its results can be considered a good approximation for the quantum behavior of mBEC[11,30].

In this article we present the results of numerical modeling of magnon tunneling between the two mBEC, located in two samples of YIG separated by a thin gap. This configuration corresponds to tunneling experiments and Josephson effect in superconductors. The overlap of the wave functions of magnon condensates occurs due to the dipole-dipole interaction in this case. The considered model gives a realistic estimate of the magnon tunneling and its experimental verification in the planned experiments will shed light on the quantum properties of mBEC.

Methods and results

The magnetization dynamics in two identical YIG square films is calculated using the open-source finite-difference micromagnetic solver MuMax^3 (see Ref.[31]). Simulations were done on the high performance platform "Zhores" based on SkolTech[32]. We simulate magnetization dynamics at zero temperature in square films with a side length $a = 5$ μm, thickness $d = 10$ nm separated by a gap with length l_{gap} Computational cell size was chosen $10 \times 10 \times 10$ nm^3 (see Fig. 1). The following magnetic parameters are used: $\mu_0 M_S = 165$ mT, $A = 3.49 \times 10^{-12}$ J/m. Crystallographic anisotropy has been neglected. The external dc magnetic field with magnitude of $B_z = 0.25$ T applied along z-axis and microwave field with an amplitude $b_{\text{rf}} = 100$ μT and frequency f excited along x-axis only in the left film. Magnons in the right film were excited only by its tunneling from the left film.

We simulate the properties of our system for different parameters, such as distance between films l_{gap}, Gilbert damping α_G, and driving frequency f. The spatial distribution of the angle of precession (a) and the phase of precession (b) along the axis x are presented in Fig. 2. These results are obtained for the RF frequency of 2.45 GHz, which corresponds to the frequency shift in the central part of the sample $\Delta\omega = 6$ GHz. This shift decreases near the edges due to the decrease in the demagnetization field. Consequently, the angle of deviation of magnetization is also reduced. The magnon tunneling from the left sample leads to a formation of mBEC in the right sample except for the large gap $l_{\text{gap}} = 500$ nm in which coherent coupling is broken and, consequently, the magnon tunneling stopped. The phase leap through the gap become larger with increasing of the distance between samples, which corresponds to a Josephson relation between the samples. The tunneling rate is proportional to the phase leap. Please take into account that the magnon BEC filling up completely the right side sample by spin current, which arise due to the gradient of phase of precession. However, for the gap of 500 nm, the magnetic tunneling speed is insufficient for mBEC formation and typical spin waves are formed. The phase rapidly rotates along the sample and is not very representitive. The profile of magon density (angle of deflection) is determined by the demagnetization factor near the gap. The local field increases and consequently,$\Delta\omega$ decreases. In these simulations $\alpha_G = 2 \times 10^{-5}$

We simulated mBEC properties at different relaxation rates. The results are shown in Fig 3. From this figure it is clear that higher damping leads to an increase in the phase gradient and the magnon flow. The magnon density and angle of deflection determined by the frequency shift $\Delta\omega$ and, consequently, by the RF frequency. In Fig. 4 shown the precession amplitude and phase for four different pumping frequencies. We see that the tunneling speed decreases with a decrease in magnon density. In addition, the relaxation rate and the magnon relaxation also decrease with the magnon density. Pay attention to the fact that for 2.40 GHz pumping the magnon density is not enough to fill all the right samples. Small artifacts near the edges are explained by the huge increase of calculation time to achieve quasi-stationary conditions for a small density of magnons.

Conclusion

Magnon BEC is a unique coherent quantum state that exists at room temperature. Traditionally, the magnetic resonance is considered in the linear approximation when MBEC is not formed. The question araises, how the existence of mBEC can be shown experimentally? This is the direct result of quantum statistics when the macroscopic amount of bosonic quasiparticles occupy the lowest level[2]. In other words, the question of the reality of mBEC with a given density of nonequilibrium magnons is equivalent to the question of the reality of quantum physics. The non-linear properties of magnetic resonance are traditionally considered in a framework of a single non-linear oscillator[33]. This model is applicable only to very small samples with the

dimensions of the order of exchange interaction or for the case of an absolutely homogeneous external field, which is not a case for general conditions. In this model, the amplitude of the resonance is proportional to the excitation power. Indeed, for a quantum model, the amplitude is proportional to the frequency shift, and does not depend on the RF power, if it is enough for mBEC formation. A complete verification of the quantum behavior of nonequilibrium magnon gas was performed in antiferromagnetic superfluid ^{3}He, the results of which were awarded by the prestigious F. London prize. An experimental verification for the quantum behavior of nonequilibrium magnon gas in YIG was described in[9].

MBEC is a very promising system for quantum calculations. The use of mBEC allows for an increase in energy scales via bosonic enhancement[34], resulting in gate operations that can be performed at a macroscopically large energy scale and can be considered as a perspective platform for quantum computing[35]. The spatial entanglement between Bose-Einstein condensates was recently considered in the review[36]. YIG samples chain with mBEC, interacting through magnon Josephson junctions, described in our article, can be viewed as a multi qubits system. The spatial distribution of mBEC at the edge of the sample is crucial for this type of qubits design. Owing to the equivalence of quantum and classical approaches for a large concentration of magnons, our calculations of the magnetic tunneling are applicable to quantum systems. Indeed, magnon transport properties for quantum and classical models are very different. In our calculations for a magnon transport in the right sample, we used a classical approach, which is equivalent to solid-body rotation. In reality, the transport phenomena should be described by supercurrent. It should result in a smoothing of phase gradient. Experimental verification of deviation from a solid body model is very important.

The other approach for magnon BEC and its application for quantum computing are demonstrated in in-plane magnetized YIG films ([28] in references there).

A very important question of the thermal limit for the magnon qubit functionality since mBEC exists even at room temperature. Thermal fluctuations may possibly be averaged for a macroscopic number of identical magnons in the condensate. Therefore, the quantum computing based on mBEC may possibly be performed even at a room temperature.

Acknowledgments

This work was financially supported by the Ministry of Science and Higher Education of the Russian Federation (Megagrant project no. 075-15-2019-1934). The authors acknowledge the use of computational resources of the Skoltech CDISE supercomputer Zhores for obtaining the results presented in this paper.

Data Availability

The data that support the findings of this study are available from the corresponding authors upon reasonable request.

References

1. Holstein, T. & Primakoff, H. Field dependence of the intrinsic domain magnetization of a ferromagnet. *Phys. Rev.* 1098 (1940).
2. Bunkov, Y. M. & Safonov, V. L. Magnon condensation and spin superfluidity. *J. Mag. Mag. Mat.* 30 (2018).
3. Flebus, B. & Tserkovnyak, Y. Entangling distant spin qubits via a magnetic domain wall. *Phys. Rev. B* **99**, 140403 (2019).
4. Sanchez-Kuntz, N. & Floerchinger, S. Spatial entanglement in interacting bose-einstein condensates. *Phys. Rev. A* **103**, 043327 (2021).
5. Mousolou, V. *et al.* Magnon-magnon entanglement and its detection in a microwave cavity. *arxiv 2106.06862* (2021).
6. Rogel-Salazar, J. The gross–pitaevskii equation and bose–einstein condensates. *Eur. J. Phys.* **34**, 247 (2013).
7. Bunkov, Y. M. & Volovik, G. E. *Spin Superfluidity and Magnon BEC* (Oxford Univ. Press, Oxford, 2013).
8. Dalfovo, F., Pitaevskii, L. & Stringari, S. Order parameter at the boundary of a trapped Bose gas. *Phys. Rev. A* **54**, 4213 (1996).
9. Bunkov, Y. M. *et al.* Quantum paradigm of the foldover magnetic resonance. *Sci. Reports* **11**, 7673 (2021).
10. Borovik-Romanov, A. S., Bun'kov, Y. M., Dmitriev, V. V. & Mukharskii, Y. M. Long-lived induction signal in superfluid ^{3}He-B. *JETP Lett.* **40**, 1033–1037 (1984).
11. Bunkov, Y. M. & Volovik, G. E. Bose-Einstein condensation of magnons in superfluid ^{3}He. *J. Low Temp Phys.* **150**, 135–144 (2008).
12. Bunkov, Y. M., Dmitriev, V. V., Mukharskiy, Y. & Tvalashvili, G. Superfluid spin current in a channal parallel to the magnetic field. *Sov. Phys. JETPh* **67**, 300 (1988).

13. Bunkov, Y. M. Spin supercurrent in ^{3}He. *Jpn. J. Appl. Phys.* **26**, 1809 (1987).

14. Borovik-Romanov, A. S., Bunkov, Y. M., Dmitriev, V. V. & Mukharskiy, Y. M. Observation of phase slippage during the flow of a spin supercurrent in ^{3}He. *JETP Lett.* **45**, 124 (1987).

15. Borovik-Romanov, A. S. *et al.* Investigation of spin supercurrents in ^{3}B. *Phys. Rev. Lett.* **62**, 1631 (1989).

16. Borovik-Romanov, A. S. *et al.* Observation of a spin supercurrent analog of the Josephson effect. *JETP Lett.* **47**, 478 (1988).

17. Borovik-Romanov, A. S. *et al.* The analog of the josephson effect in the spin supercurrent. *J. de Physique* **49 (C8)**, 2067 (1988).

18. Borovik-Romanov, A. S., Bunkov, Y. M., Dmitriev, V. V., Mukharskiy, Y. M. & Sergatskov, D. A. Observation of vortex-like spin supercurrent in ^{3}He-B. *Phys. B* **165**, 649–650 (1990).

19. Bunkov, Y. M. & Volovik, G. E. Spin vortex in magnon bec of superfluid ^{3}He-B. *Phys. C* **468**, 600 (2008).

20. Bunkov, Y. M. Spin supercurrent and coherent spin precession. *J. Phys.:Cond. Mat.* **21**, 164201 (2009).

21. Bunkov, Y. M. & Volovik, G. E. Magnon Bose-Einstein condensation and spin superfluidity. *J. Phys.: Cond. Mat.* **22**, 164210 (2010).

22. Autti, S. *et al.* Ac josephson effect between two superfluid time crystals. *Nat. materials* **20**, 171–174 (2020).

23. Bunkov, Y. M. *et al.* High T_c spin superfluidity in antiferromagnets. *Phys. Rev. Lett.* **108**, 177002 (2012).

24. Alakshin, E. M. *et al.* Bose-Einstein condensation in antiferromagnets at low temperatures. *J. Phys. Conf.* **568**, 042001 (2014).

25. Abdurakhimov, L. V. *et al.* Nonlinear NMR and magnon BEC in antiferromagnetic materials with coupled electron and nuclear spin precession. *Phys. Rev. B* **97**, 024425 (2018).

26. Bunkov, Y. M., Klochkov, A. V., Safin, T. R., Safiullin, K. R. & Tagirov, M. S. Nonresonance excitation of magnon Bose-Einstain condensation in $MnCO_3$. *JETP Lett.* **109**, 43 (2019).

27. Serga, A. A. *et al.* Bose-Einstein condensation in an ultra-hot gas of pumped magnons. *Nat. Commun.* **5**, 3452 (2014).

28. Noack, T. B. *et al.* Evolution of room-temperature magnon gas toward coherent Bose-Einstein condensate. *arXiv:2101.07890* (2021).

29. Vetoshko, P. M. *et al.* Bose condensation and spin superfluidity of magnons in a perpendicularly magnetized film of yttrium iron garnet. *JETP Lett.* **112**, 299 (2020).

30. Bunkov, Y. M. Magnonics and supermagnonics. *Spin* **9**, 1940005 (2019).

31. Vansteenkiste, A. *et al.* The design and verification of Mumax3. *AIP Adv.* **4**, 107133 (2014).

32. Zacharov, I. *et al.* Zhores — petaflops supercomputer for data-driven modeling, machine learning and artificial intelligence installed in Skolkovo Institute of Science and Technology. *Open Eng.* **9** (2019).

33. Anderson, P. W. & Suhl, H. Instability in the motion of ferromagnets at high microwave power levels. *Phys. Rev.* **100**, 1788 (1955).

34. Byrnes, T., Wen, K. & Yamamoto, Y. Macroscopic quantum computation using bose-einstein condensates. *Phys. Rev. A* **85**, 040306 (2012).

35. Bunkov, Y. M. Quantum magnonics. *JETP* **131**, 18–28 (2020).

36. Sánchez-Kuntz, N. & Floerchinger, S. Spatial entanglement in interacting bose-einstein condensates. *Phys. Rev. A* **103**, 043327 (2021).

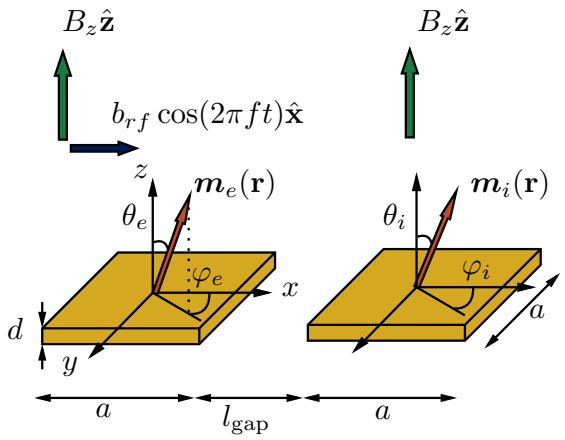

Figure 1. Sketch of the system studied. We considered two samples of square YIG films with the same sides $a = 5$ μm, and thicknesses $d = 10$ nm. External dc magnetic field with magnitude of $B_z = 0.25$ T applied perpendicular to the film planes. The in-plane rf field with an amplitude $b_{\text{rf}} = 100$ μT and frequency f applied only in the left film and excites magnetization $\boldsymbol{m}_e(\mathbf{r})$. The induced precession of vector of magnetization $\boldsymbol{m}_i(\mathbf{r})$ in the right film arises due to magnetodipolar interaction throw the gap.

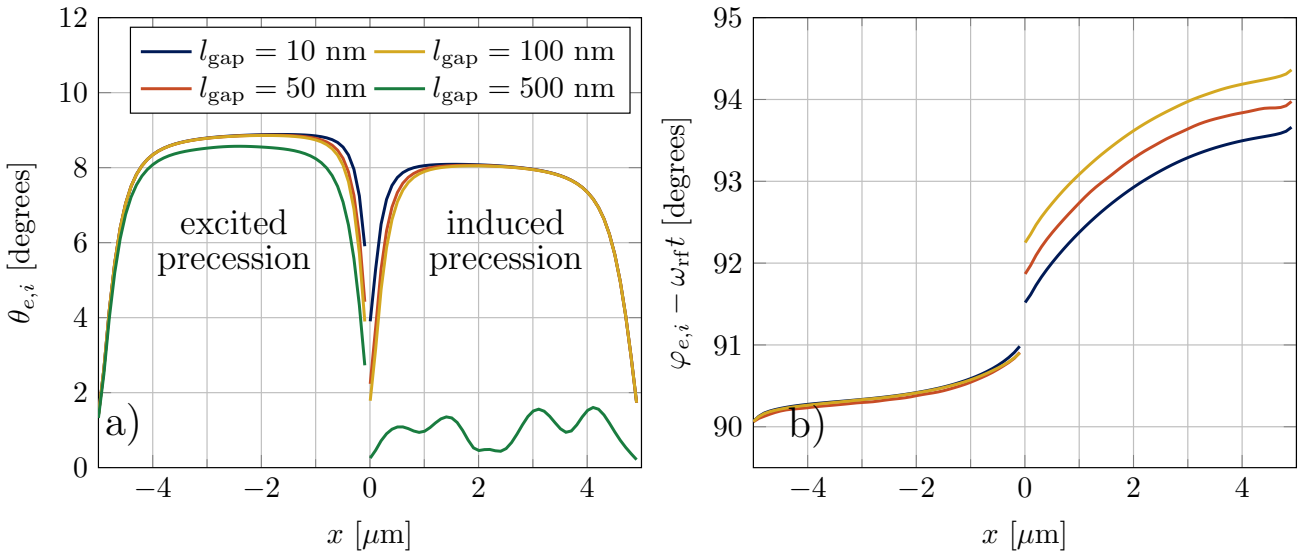

Figure 2. The spatial destribution of the angle of precession (a) and the phase of precession (b) for the RF puming at a frequency f = 2.45 GHz, which corresponds to frequency shift $\Delta\omega = 6$ GHz at different gap lengths. For $l_{\text{gap}} = 500$ nm the coherent coupling is broken and, consequently, the magnon tunneling stopped. In these simulations $\alpha_G = 2 \times 10^{-5}$

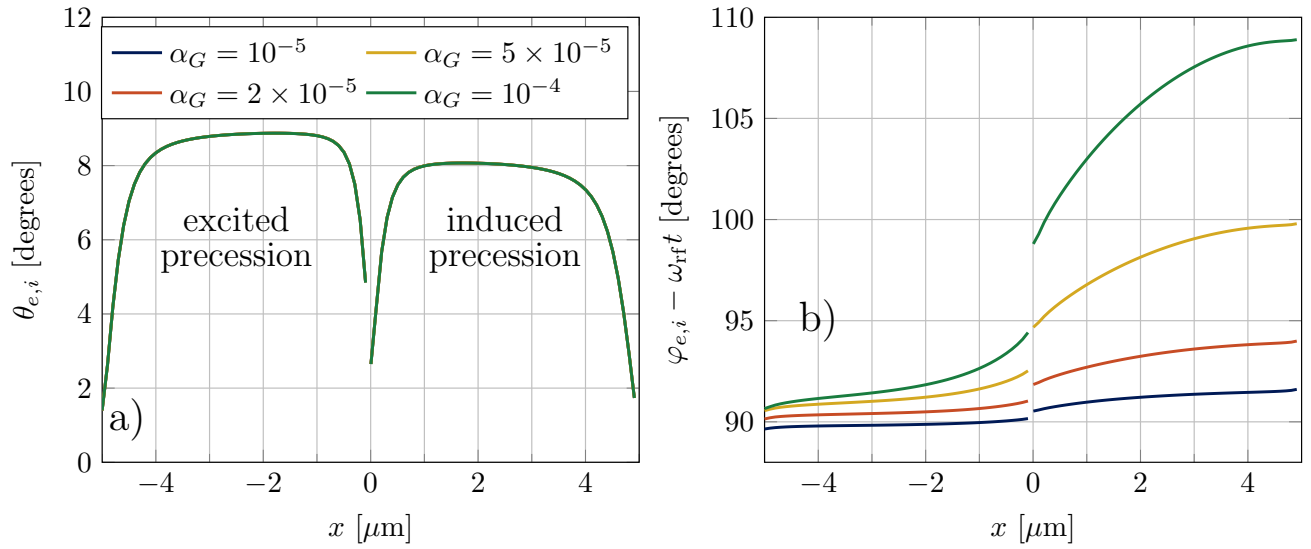

Figure 3. The spatial destribution of the angle of precession (a) and the phase of precession (b) at different magnon relaxation rate for the RF puming at a frequency 2.45 GHz. Solid line correspond to $\alpha_G = 10^{-5}$, dotted line $\alpha_G = 2 \times 10^{-5}$, dashed line $\alpha_G = 5 \times 10^{-5}$, dashdotted line $\alpha_G = 10^{-4}$. The gap $l_{\mathrm{gap}} = 30$ nm. Note, that the profile of magnon density does not depend from the relaxation rate at this parameters.

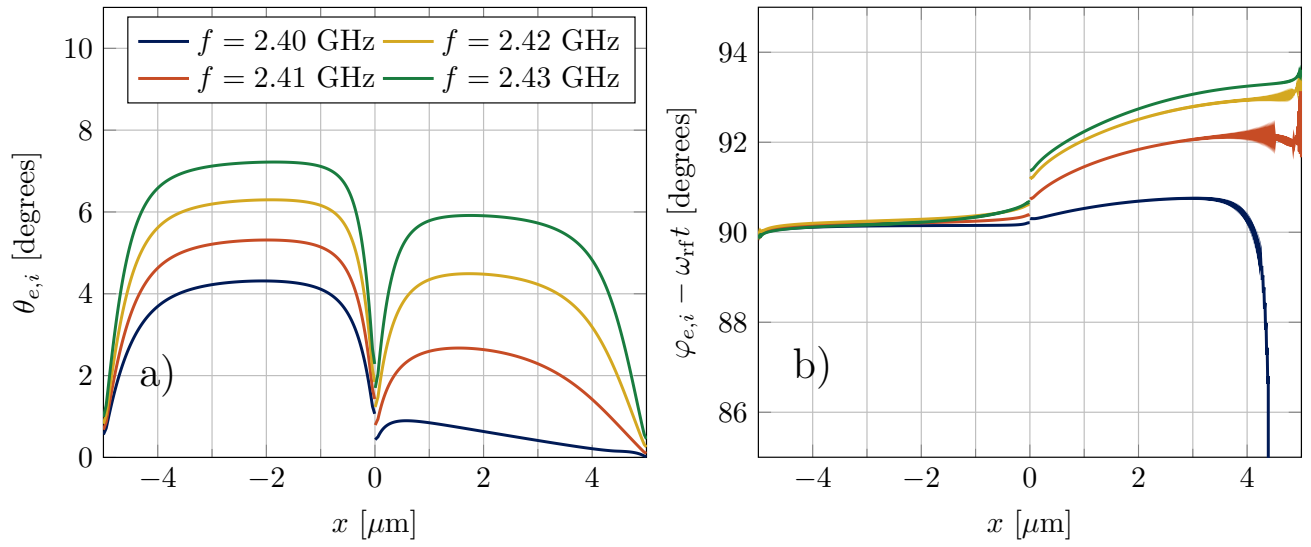

Figure 4. The spatial destribution of the angle of precession (a) and the phase of precession (b) at different RF puming frequency. Here the magnet density determines by the parameter $\Delta\omega$, which is 1 GHz, 2 GHz, 3 GHz and 4 GHz, respectively. For the case of 2.40 GHz, the magnon density is not enough to fill the entire right sample. The gap $l_{\mathrm{gap}} = 30$ nm.